
Dynamical Stability of the Laplace Resonance

Giuseppe Pucacco

the date of receipt and acceptance should be inserted later

Abstract We analyse the stability of the *de Sitter equilibria* in multi-resonant planetary systems. The de Sitter equilibrium is the dynamical state of the Laplace resonance in which all resonant arguments are librating. The sequence of equilibria exists all along the possible states balancing resonance offsets and forced eccentricities. Possible additional new-de Sitter equilibria may exist when at least one of the forced eccentricities is large (the paradigmatic case is Gliese-876). In the present work, these families of equilibria are traced up to crossing exact commensurability, where approximate first-order solutions diverge. Explicit exact location of the equilibria are determined allowing us to verify the Lyapunov stability of the standard de Sitter equilibrium and of the stable branches of the additional ones.

Keywords Celestial mechanics · Planets and satellites: dynamical evolution and stability · Methods: analytical · Methods: numerical

1 Motivations

In the catalog of exo-planetary systems, there is a small but constantly growing set of *multi-resonant* items, namely planetary systems with three or more commensurate periods. For example, for 1+3-body systems, there is a certain number of them with period ratios given by $n_2/n_1 = (k_1 - 1)/k_1$ and $n_3/n_2 = (k_2 - 1)/k_2$, $k_1, k_2 \in \mathbb{Z}$ (Pichierri et al. 2019), configurations that we can call *Laplace-like resonances* as generalisations of the classical Galilean-system dynamics (Celletti et al. 2019). The standard Laplace resonance is produced by $k_1 = k_2 = 2$.

Since the formation scenarios and subsequent migration of just formed planets favour the birth of resonant chains, we would expect that the fraction of systems trapped in such states could be quite high, especially for systems in which *Super-Earths* or *mini-Neptunes* are abundant (Petit et al. 2020). However this is not the case, since the examples of these multi-resonant systems amount to some tens over a total

G. Pucacco
Dipartimento di Fisica and INFN – Sezione di Roma II, Università di Roma “Tor Vergata”,
Via della Ricerca Scientifica, 1 - 00133 Roma
E-mail: pucacco@roma2.infn.it

of a few thousand systems. Both for transiting planets and for radial-velocity ones, the period ratios are known with high precision, therefore the lack of such configurations seems to be not an arti-fact (Charalambous et al. 2023; Nagpal et al. 2024). A simple explanation of this phenomenon could be that these systems, after the disappearance of the proto-planetary disk, are quite prone to dynamical instabilities making them short lived systems (Izidoro et al. 2017). However, as a matter of fact, the analysis of the stability of Laplace-like resonant configurations still present some problematic issues. In fact, numerical simulations appear to show that these states are indeed dynamically stable for initial conditions quite close to resonant equilibria and therefore other instability mechanisms such as higher-order resonances have been invoked (Pichierri and Morbidelli 2020; Goldberg et al. 2022).

However, no analytical proof of dynamical stability is available and, even more, model predictions are at odds with numerical simulations. In particular, a paradox concerning stability has to be solved: classical works (Yoder and Peale 1981; Henrard 1982) predict *instability* beyond a certain threshold of proximity to the resonance. On the other hand, direct numerical integrations point out dynamical stability. Pichierri and Morbidelli (2020) claim that “*the purely resonant system ... with initial condition at vanishing amplitude around a resonant equilibrium point is (Lyapunov) stable for all planetary masses*”. Therefore, it seems that a thorough analysis of the stability nature of the standard Laplace resonance is worthy of being endeavored, also in view of the renovated interest in the Galilean system (Ferraz-Mello 2021; Lainey et al. 2006; Cappuccio et al. 2020; Lari and Saillenfest 2024).

In the present work we see how to reconcile these predictions by exploiting an accurate location of the ‘de Sitter-Sinclair’ equilibria. This result is obtained with a more effective way of characterising the proximity to the resonance. In fact, we will follow the sequence of equilibria all along the possible states in which resonance offsets and forced eccentricities balance, whereas the usual reckoning of Laplace equilibria proceeds by assuming small forced eccentricities (Sinclair 1975; Henrard 1984; Broer and Hanßmann 2016). However, if the resonance offsets are small, this assumption leads to an inconsistency and equilibrium solutions may well be characterised by moderate or even large eccentricities. The determination of these equilibrium configurations has to be extended to a more generic setting; this radically modifies the nature of the equilibria and also leads to the bifurcation of ‘new-de Sitter’ families of equilibria (Pucacco 2021). In this case, under certain conditions, a saddle-node bifurcation generates a stable/unstable pair of additional critical points. The stability analysis will therefore be extended also to these equilibria, of which a paradigmatic example is the GJ-876 exo-planetary system.

The plan of the paper is as follows: in Sect.2 we remind the basic Hamiltonian of the multi-resonant self-gravitating system; in Sect.3 we present the new solutions for the equilibria and analyse the conditions for their linear stability and bifurcations; in Sect.4 we discuss normalisation around these equilibria; in Sect.5 we apply these results to the examples of the Galilean system and of GJ-876; in Sect.6 we conclude with some general remarks.

2 The dynamical model

Here we want to describe the main properties of the Laplace-resonant dynamics. When considered as a *relative equilibrium* of a reduced Hamiltonian system, the de Sitter

equilibrium is the dynamical state of the Laplace resonance in which all resonant arguments are librating. In real systems (e.g. the standard case characterising the Galilean system), since one of the free eccentricities is larger than the forced one, usually the corresponding argument rotates. However, this state shares the same dynamical properties as the de Sitter one.

One of the easiest way to characterise the resonant regime is to exploit a simple model of the libration of the (generalised) Laplace angle. Therefore, the tool we should construct is a normal form giving the phase plot of a (possibly integrable) reduced dynamics. Preliminary steps for this are the introduction of a suitable coordinate set and the reduction of the Hamiltonian model. Referring to the set of canonical coordinates useful for this purpose, we perform some modification with respect to the standard approach adopted when describing the Galilean system (Henrard 1984; Malhotra 1991).

The basis of the work is a simplified model aimed at capturing the essential features of the true system. We consider a planar system in which 3 relatively small bodies with orbital elements $a_j, e_j, \lambda_j, p_j, j = 1, 2, 3$, revolve around a ‘large’ central one. The model Hamiltonian is then given by the Keplerian part plus the resonant terms describing the coupling of the ‘satellites’

$$H(L_j, P_j, \lambda_j, p_j) = H_{kep} + H_{res}, \quad (j = 1, 2, 3), \quad (1)$$

which survive after averaging with respect to fast angle-combinations. Therefore, the modified Delaunay variables L_j, P_j, λ_j, p_j can be interpreted as the osculating elements of the starting model Hamiltonian (Charalambous et al. 2018). In the present section we illustrate the structure of Hamiltonian (1) and the canonical transformations useful to unveil its dynamics.

2.1 Keplerian part

The Keplerian part of the Hamiltonian is given by:

$$H_{kep} = -\frac{1}{2} \sum_{j=1}^3 \frac{M_j^2 \mu_j^3}{L_j^2} \quad (2)$$

where we define

$$\begin{aligned} M_1 &= m_0 + m_1, & \mu_1 &= \frac{m_0 m_1}{M_1}, \\ M_2 &= M_1 + m_2, & \mu_2 &= \frac{M_1 m_2}{M_2}, \\ M_3 &= M_2 + m_3, & \mu_3 &= \frac{M_2 m_3}{M_3}. \end{aligned} \quad (3)$$

Units are such that Newton gravitation constant is set to unity. By expanding H_{kep} up to second order with respect to the nominal resonant values \bar{L}_j we get:

$$H_{kep} = \sum_{j=1}^3 \left(\bar{n}_j (L_j - \bar{L}_j) - \frac{3}{2} \eta_j (L_j - \bar{L}_j)^2 \right), \quad (4)$$

where

$$\bar{n}_j = \sqrt{\frac{M_j}{\bar{a}_j^3}} = \frac{M_j^2 \mu_j^3}{\bar{L}_j^3}, \quad \eta_j = \frac{\bar{n}_j}{\bar{L}_j}. \quad (5)$$

We use exact-commensurability conditions in order to compute nominal values, following Batygin and Morbidelli (2013b) and Pucacco (2021), so that \bar{a}_j are the normalised resonant semi-axes values, \bar{n}_j the nominal mean motions and, in the general case of first-order resonances,

$$\begin{aligned} k_1 \bar{n}_2 &= (k_1 - 1) \bar{n}_1, & k_1 &= 2, 3, \dots \\ k_2 \bar{n}_3 &= (k_2 - 1) \bar{n}_2, & k_2 &= 2, 3, \dots \end{aligned} \quad (6)$$

Using these relations we can compute the nominal resonant values, in particular this is the choice for the nominal values \bar{L}_j and η_j .

2.2 The resonant coupling terms

The disturbing function, as usual in the case of first-order resonances (Ferraz-Mello 2007; Papaloizou 2015; Pichierri et al. 2019), is limited to low-order terms in the expansion in the eccentricities. After averaging with respect to non-resonant ‘fast’ angles, we obtain terms of the form

$$\begin{aligned} H_{res}^{(1)} &= -\frac{m_1 m_2}{a_2} (f_{12,1} e_1 \cos(k_1 \lambda_2 - (k_1 - 1) \lambda_1 + p_1) \\ &\quad + f_{12,2} e_2 \cos(k_1 \lambda_2 - (k_1 - 1) \lambda_1 + p_2)) \\ &\quad - \frac{m_2 m_3}{a_3} (f_{23,1} e_2 \cos(k_2 \lambda_3 - (k_2 - 1) \lambda_2 + p_2) \\ &\quad + f_{23,2} e_3 \cos(k_2 \lambda_3 - (k_2 - 1) \lambda_2 + p_3)) \end{aligned} \quad (7)$$

for the first-order terms and

$$\begin{aligned} H_{res}^{(2)} &= -\frac{m_1 m_2}{a_2} (f_{12,6} e_1 e_2 \cos(p_1 - p_2) + f_{12,5} e_1 e_2 \cos(2k_1 \lambda_2 - 2(k_1 - 1) \lambda_1 + p_1 + p_2) \\ &\quad + f_{12,3} e_1^2 \cos(2k_1 \lambda_2 - 2(k_1 - 1) \lambda_1 + 2p_1) + f_{12,4} e_2^2 \cos(2k_1 \lambda_2 - 2(k_1 - 1) \lambda_1 + 2p_2)) \\ &\quad - \frac{m_2 m_3}{a_3} (f_{23,6} e_2 e_3 \cos(p_2 - p_3) + f_{23,5} e_2 e_3 \cos(2k_2 \lambda_3 - 2(k_2 - 1) \lambda_2 + p_2 + p_3) \\ &\quad + f_{23,3} e_2^2 \cos(2k_2 \lambda_3 - 2(k_2 - 1) \lambda_2 + 2p_2) + f_{23,4} e_3^2 \cos(2k_2 \lambda_3 - 2(k_2 - 1) \lambda_2 + 2p_3)) \\ &\quad - \frac{m_1 m_3}{a_3} (f_{13,4} e_1 e_3 \cos(p_1 - p_3)), \end{aligned} \quad (8)$$

for the 2nd-order terms. The Laplace coefficients $f_{ij,\nu}$, $i, j = 1, 2, 3$, $\nu = 1, \dots, 6$, are quantities of order one weakly dependent on the semi-major axis ratios (Murray and Dermott 2000).

2.3 Variables adapted to the resonance

Let us consider the resonance defined by (6). In order to implement the location of relative equilibria and the evaluation of their stability, we introduce a new set of canonical variables *adapted* to the first-order resonance. We closely follow the derivation in Pucacco (2021) generalising for completeness to other first-order resonances.

The new set of coordinates is provided by the transformation

$$(L_j, P_j, \lambda_j, p_j), j = 1, 2, 3 \longrightarrow (Q_\nu, q_\nu), \nu = 1, \dots, 6.$$

The new actions Q_ν are given by:

$$\begin{aligned}
Q_1 &= P_1 \\
Q_2 &= P_2 \\
Q_3 &= P_3 \\
Q_4 &= \frac{k_1}{3(k_1-1)}L_1 + \frac{L_2}{3} + \frac{L_3}{3k_2}(k_2-4) \\
Q_5 &= \frac{k_1+k_2-1}{3(k_1-1)}L_1 + \frac{L_2}{3} + \frac{1}{3}(k_2-1)(P_1+P_2+P_3) \\
Q_6 &= L_1+L_2+L_3-P_1-P_2-P_3.
\end{aligned} \tag{9}$$

and the new angles q_ν are

$$\begin{aligned}
q_1 &= k_1\lambda_2 - (k_1-1)\lambda_1 + p_1 \\
q_2 &= k_1\lambda_2 - (k_1-1)\lambda_1 + p_2 \\
q_3 &= k_1\lambda_2 - (k_1-1)\lambda_1 + p_3 \\
q_4 &= (k_1\lambda_2 - (k_1-1)\lambda_1) - (k_2\lambda_3 - (k_2-1)\lambda_2) \\
&= (1-k_1)\lambda_1 + (k_1+k_2-1)\lambda_2 - k_2\lambda_3 \\
q_5 &= \frac{4(k_1-1)}{k_2}\lambda_1 - \frac{4(k_1-1)+k_2}{k_2}\lambda_2 + \lambda_3 \\
q_6 &= \frac{(k_1-1)(k_2-4)}{3k_2}\lambda_1 \\
&\quad - \frac{(k_2-4)(k_1+k_2-1)}{3k_2}\lambda_2 + \frac{1}{3}(k_2-1)\lambda_3.
\end{aligned} \tag{10}$$

In the model at hand, angles q_5, q_6 are *cyclic* (they do not appear anymore in the Hamiltonian (1)) and this implies that Q_5 and Q_6 are exact integrals of motion of H .

$$Q_6 = \sum_{j=1}^3 (L_j - P_j)$$

is the *total angular momentum* of the system. We can also use the linear combination

$$Q_L = 3Q_5 + (k_2-1)Q_6 = \frac{k_1k_2}{k_1-1}L_1 + k_2L_2 + (k_2-1)L_3$$

which is a *scaling invariant* (Batygin and Morbidelli (2013a), also dubbed *spacing parameter* by Michtchenko et al. (2008)). Introducing the *angular momentum deficit* (Laskar and Petit 2017)

$$\Gamma = \sum_{j=1}^3 P_j = \sum_{j=1}^3 Q_j, \tag{11}$$

the inverse transformation for the L_j actions is given by:

$$\begin{aligned}
L_1 &= -(k_1-1)\Gamma - (k_1-1)Q_4 \\
&\quad + \frac{4(k_1-1)}{k_2}Q_5 + \frac{(k_1-1)(k_2-4)}{3k_2}Q_6 \\
L_2 &= k_1\Gamma + (k_1+k_2-1)Q_4 \\
&\quad - \frac{4k_1+k_2-4}{k_2}Q_5 - \frac{(k_2-4)(k_1+k_2-1)}{3k_2}Q_6 \\
L_3 &= -k_2Q_4 + Q_5 + \frac{1}{3}(k_2-1)Q_6.
\end{aligned} \tag{12}$$

The set of variables adapted to the resonance given by (9)-(10), when compared with the original Henrard-Malhotra one (Henrard 1984; Malhotra 1991), has the advantage that the action Q_4 , conjugated to the Laplace argument q_4 , does not depend on the eccentricities. This fact allows us to decouple the dynamical description of the Laplace libration from those of the free eccentricities around the forced ones, as will be clear with the use of the normal form. We remark that the transformation (9)-(10) is equivalent to that introduced by Delisle (2017). Still, the main difference relies on the choice of Q_4 conjugated with the Laplace argument. The conserved quantities in the two approaches are connected by linear relations.

The model Hamiltonian can therefore be expressed as

$$H(Q_a, q_a; Q_5, Q_6) = \sum_{n=0}^{\infty} H_n(Q_a, q_a), \quad a = 1, \dots, 4, \quad (13)$$

where the first three terms in the Hamiltonian (13) are

$$H_0 = \kappa_1 \Gamma + \kappa_4 Q_4, \quad (14)$$

$$H_1 = -\frac{3}{2} A \Gamma^2 - 3B \Gamma Q_4 - \frac{3}{2} C Q_4^2, \quad (15)$$

$$H_2 = -\alpha \sqrt{2Q_1} \cos q_1 - \beta_1 \sqrt{2Q_2} \cos q_2 \\ - \beta_2 \sqrt{2Q_2} \cos(q_2 - q_4) - \gamma \sqrt{2Q_3} \cos(q_3 - q_4), \quad (16)$$

where

$$\Gamma = Q_1 + Q_2 + Q_3.$$

Terms of higher order in the expansion $H_n, n > 2$ can be added, but we will only use them in some later applications. The frequencies $\kappa_1(Q_5, Q_6), \kappa_4(Q_5, Q_6)$, are

$$\kappa_1 = \kappa_{11} Q_5 + \kappa_{12} Q_6, \quad (17)$$

$$\kappa_4 = \kappa_{41} Q_5 + \kappa_{42} Q_6, \quad (18)$$

where

$$\kappa_{11} = 12 \frac{(k_1 - 1)^2}{k_2} \eta_1 + \frac{3k_1(k_2 + 4k_1 - 4)}{k_2} \eta_2 \quad (19)$$

$$\kappa_{12} = \frac{(k_2 - 4)(k_1 - 1)^2}{k_2} \eta_1 + \frac{k_1(k_2 - 4)(k_1 + k_2 - 1)}{k_2} \eta_2 \quad (20)$$

$$\kappa_{41} = \frac{12(k_1 - 1)^2}{k_2} \eta_1 + \\ \frac{3(4k_1 + k_2 - 4)(k_1 + k_2 - 1)}{k_2} \eta_2 + 3k_2 \eta_3 \quad (21)$$

$$\kappa_{42} = \frac{(k_1 - 1)^2(k_2 - 4)}{k_2} \eta_1 + \\ \frac{(k_1 + k_2 - 1)^2(k_2 - 4)}{k_2} \eta_2 + k_2(k_2 - 1) \eta_3. \quad (22)$$

The Keplerian expansion parameters A, B, C are given by

$$A = (k_1 - 1)^2 \eta_1 + k_1^2 \eta_2 \\ B = (k_1 - 1)^2 \eta_1 + k_1(k_1 + k_2 - 1) \eta_2 \\ C = (k_1 - 1)^2 \eta_1 + (k_1 + k_2 - 1)^2 \eta_2 + k_2^2 \eta_3 \quad (23)$$

and the coupling parameters $\alpha, \beta_1, \beta_2, \gamma$ are defined as usual

$$\begin{aligned}
 \alpha &= \bar{m}_2 \epsilon_2 \frac{f_{12,1}}{\bar{L}_2^2 \sqrt{\bar{L}_1}} \\
 \beta_1 &= \bar{m}_2 \epsilon_2 \frac{f_{12,2}}{\bar{L}_2^2 \sqrt{\bar{L}_2}} \\
 \beta_2 &= \bar{m}_2 \bar{m}_3^2 \epsilon_3 \frac{f_{23,1}}{\bar{L}_3^2 \sqrt{\bar{L}_2}} \\
 \gamma &= \bar{m}_2 \bar{m}_3^2 \epsilon_3 \frac{f_{23,2}}{\bar{L}_3^2 \sqrt{\bar{L}_3}}
 \end{aligned} \tag{24}$$

with the specific value of the Laplace coefficients and the definitions

$$\begin{aligned}
 \epsilon_k &= \frac{m_k}{m_0}, \quad k = 1, 2, 3 \\
 \bar{m}_j &= \frac{m_j}{m_1} = \frac{\epsilon_j}{\epsilon_1}, \quad j = 2, 3.
 \end{aligned} \tag{25}$$

This set has to be considered as a ‘fixed’ set of constant parameters determined by physical quantities (e.g. the masses) and the nominal resonant variables. Rather, Q_5 and Q_6 depend on *initial conditions* L_j^0, Q_j^0 , $j = 1, 2, 3$, which clearly are close but *not* coinciding with the nominal ones $L_j = \bar{L}_j, Q_j = 0$. However, the osculating elements used to compute the integrals of motion Q_5, Q_6 may well be substantially displaced with respect to those corresponding to exact commensurability. Choosing for example almost circular orbits would imply semi-major axis ratios sensibly different from the nominal ones as suggested by typical formation scenario driven by dissipative interactions (Goldberg et al. 2022; Nagpal et al. 2024).

From the analytical point of view, (13) is a *reduced Hamiltonian* (Abraham and Marsden 1987). Its dynamics occur on a 4-DoF (Degrees of Freedom) reduced phase-space (Henrard 1984; Broer and Hanßmann 2016). In particular, its critical points provide equilibria which, when mapped back through the inverse transformation (12), in combination with (9), give periodic orbits. These orbits inherit the stability nature of the parent equilibrium. In the next section we will introduce a unique parameter of ‘proximity’ to the resonance which allows us to properly parametrise the status of the reduced systems. We remark that the ordering of the terms in (13) reflects only their meaning and origin. The actual ordering in the Hamiltonian expansions and the normal form construction will be established case by case on the basis of suitable assumptions.

3 Equilibria of the Laplace-resonance

Historically, the description of the Laplace-resonant state as an equilibrium can be attributed to de Sitter (1909, 1931). The approach was later extended by Sinclair (1975) and discussed in several other works. New ‘de Sitter-Sinclair’ equilibria may appear with different apsidal combinations and possibly higher forced eccentricities (Pucacco 2021; Wang et al. 2024).

We have a reduced 4-DoF Hamiltonian vector field associated to (13). Fixed points of this field give the equilibria of the system. In the first-order (in eccentricity) case, an explicit expression of these critical points is straightforward (Sinclair 1975; Pucacco 2021). It would be nice to have analytical solutions in the general case, since they

provide clues for a full understanding of what is going on. We remark that from now on, we limit all expressions to the ‘standard’ Laplace-resonance with

$$k_1 = k_2 = 2$$

so that, as usual

$$q_1 = 2\lambda_2 - \lambda_1 + p_1, \quad Q_1 = P_1, \quad (26)$$

$$q_2 = 2\lambda_2 - \lambda_1 + p_2, \quad Q_2 = P_2, \quad (27)$$

$$q_3 = 2\lambda_2 - \lambda_1 + p_3, \quad Q_3 = P_3, \quad (28)$$

$$q_4 = 3\lambda_2 - 2\lambda_3 - \lambda_1, \quad Q_4 = \frac{1}{3}(2L_1 + L_2 - L_3), \quad (29)$$

$$q_5 = \lambda_1 - \lambda_3, \quad Q_5 = \frac{1}{3}(3L_1 + L_2 + \Gamma), \quad (30)$$

$$q_6 = \lambda_3, \quad Q_6 = L_1 + L_2 + L_3 - \Gamma. \quad (31)$$

We remark that the third resonant angle is the only one differing from the standard convention in which is used the combination $q_3 - q_4 = 2\lambda_3 - \lambda_2 + p_3$. Moreover we can define the ‘scaling parameter’, which is the integral of motion

$$Q_L = 4L_1 + 2L_2 + L_3 = 3Q_5 + Q_6. \quad (32)$$

3.1 Resonance proximity parameter

In order to highlight the dynamics of the Laplace libration we need to make a further simplification of our starting model. A standard way to simplify the structure of the Hamiltonian is that of constructing a ‘normal form’. We then investigate the equilibria of the models introduced above and proceed with normalising around them. We remark that, along the lines pioneered by Henrard (1984), the librational normal form is not limited to small amplitudes. Before approaching this task, we note that the ordering implicit in (14-16) is not necessarily appropriate. As a matter of fact, by using a suitable book-keeping parameter ε , we can rearrange the terms of the reduced Hamiltonian denoting it as

$$\mathcal{H}_0 + \varepsilon\mathcal{H}_1 + \varepsilon^2\mathcal{H}_2 + \dots,$$

with the freedom of ordering terms on the basis of specific assumptions.

Let us assume that Q_4 (by construction) and A, B, C (by definition) are quantities of order 1. For typical configurations characterised by small eccentricities (e.g. in the Galilean system) we have that $\sqrt{Q_j} \sim e_j \sim 10^{-3}$; the same order of magnitude can be associated to the coupling parameters α, β_1 , etc. On these bases, a reasonable ordering is

$$\mathcal{H}_0 = \kappa_4 Q_4 - \frac{3}{2} C Q_4^2, \quad (33)$$

$$\mathcal{H}_1 = (\kappa_1 - 3BQ_4)\Gamma + \mathcal{H}_{res}^{(1)}, \quad (34)$$

$$\mathcal{H}_2 = -\frac{3}{2} A \Gamma^2, \quad (35)$$

where $\mathcal{H}_{res}^{(1)}$ is the resonant term (16) expressed in the new variables. However, this choice, which essentially embodies the assumptions performed in previous works (Sinclair 1975; Yoder and Peale 1981; Henrard 1984), is all the less acceptable the further

the eccentricity grows. If eccentricities are, say, one order of magnitude larger, a more sensible ordering is

$$\mathcal{H}_1 = (\kappa_1 - 3BQ_4)\Gamma - \frac{3}{2}A\Gamma^2, \quad (36)$$

$$\mathcal{H}_2 = \mathcal{H}_{res}^{(1)}. \quad (37)$$

This choice will allow us to get more accurate locations of the equilibria, even if at the price of a somewhat more complicated algebra.

Before proceeding to this task, let us perform a preliminary shift which permits an effective strategy to describe the resonance. We assume that, projecting the libration of the system around the equilibrium on the phase-space planes (Q_a, q_a) , $a = 1, \dots, 4$, we get oscillations of the conjugate pair (Q_4, q_4) . We reserve to check this assumption with the normal form construction of Sect.4. Therefore, we assume that Q_4 oscillates with small amplitude around an equilibrium value that, at first order, can be approximated by exploiting the zero-order term \mathcal{H}_0 . We get:

$$\dot{q}_4 = 0 \rightarrow \frac{\partial \mathcal{H}_0}{\partial Q_4} = 0 \rightarrow Q_4^{(0)} = \frac{\kappa_4}{3C}.$$

Therefore we can introduce a new ‘small’ variable

$$\Lambda = Q_4 - Q_4^{(0)} \quad (38)$$

and assume that Λ too is of order ε . The first-order term (36) in the Hamiltonian can then be rewritten as

$$\mathcal{H}_1 = \omega\Gamma - \frac{3}{2} \left(A\Gamma^2 + 2B\Lambda\Gamma + C\Lambda^2 \right), \quad (39)$$

where

$$\omega(Q_5, Q_6) \doteq \kappa_1 - 3BQ_4^{(0)} = \kappa_1 - \frac{B}{C}\kappa_4, \quad (40)$$

is a frequency which has a relevant role in the de Sitter dynamics. Since it can profitably be used as a reliable way to measure the distance of the system from exact resonance, we call it *resonance proximity parameter* adopting the same expression introduced by Batygin (2015) in the case of two resonant planets. By using (17-18) we get

$$\omega = \frac{3}{C} [(\eta_1\eta_2 + 2\eta_1\eta_3 + 4\eta_2\eta_3)Q_L - (\eta_1\eta_2 + 4\eta_1\eta_3 + 16\eta_2\eta_3)Q_6], \quad (41)$$

but, recalling that $L_j = n_j/\eta_j$ and

$$Q_L = 4L_1 + 2L_2 + L_3, \quad Q_6 = L_1 + L_2 + L_3 - \Gamma,$$

it is very enlightening to express it in terms of direct observables

$$\omega = \frac{1}{C} [(C - B)(2n_2 - n_1) + B(2n_3 - n_2) + 2CK\Gamma], \quad K \doteq \frac{3}{2C}(AC - B^2) \quad (42)$$

and delve into its properties with some more details.

As dynamical and astronomical evidence suggest (Pichierri et al. 2019; Charalambous et al. 2023), both ‘resonance offsets’ $2n_2 - n_1$ and $2n_3 - n_2$ are most often negative quantities. Moreover, in the case of almost circular orbits, the angular momentum deficit Γ is quite small. Therefore, reminding the ordering $C > B > 0$ and the condition $K \sim |\mathcal{O}(1)|$, it is natural to consider the proximity parameter (42) as

a negative quantity well distinct from zero. This is precisely the assumption at the basis of the classical works by Sinclair (1975) and Yoder and Peale (1981) leading to first-order estimates for the equilibria (Pucacco 2021).

However, we remark that, as a matter of principle, ω can be chosen quite arbitrarily in order to produce a whole family of models. In fact, we observe that $\omega(Q_5, Q_6)$ may well vanish and even become positive. Let us demonstrate this statement from a purely mechanical point of view. After the canonical transformation (26)-(31), the original 6-DoF system is *reduced* to a 4-DoF Hamiltonian system parametrically dependent on Q_5, Q_6 . We can indeed imagine initial conditions either produced from a particular previous evolution or even concocted at art which provide values compatible with $\omega \simeq 0$. There are at least two possibilities, not mutually excluding: mean motions can be close to exact commensurability with eccentricities remaining small or, on the other hand, both resonance offsets may stay negative and large with at least one of the forced eccentricities much larger than usual. In both these cases, the proximity parameter may vanish and even become positive.

The sequence of equilibria is then the set of states balancing resonance offsets and forced eccentricities. In the following, we will analyse these cases and show that they are indeed concrete possibilities useful in applications. We stress that, whatever these cases occur, they correspond to some given values of starting L_j^0, Q_j^0 and, in turn, of Q_5, Q_6 which uniquely specify a reduced system (in addition to physical parameters).

Actually, the simplification achieved considering a one-parameter family can also be achieved by normalising action variables by one of the constant of motion (usually the spacing parameter Q_L , as done e.g. in Couturier et al. (2022)). Using ω as a proximity parameter to the resonance has the advantage to maintain a greater generality in the description of the dynamics.

3.2 Equilibrium solutions and the bifurcations of the ‘New-de Sitter’ equilibria

We can now determine the equilibrium sequence keeping, as in (39) also the quadratic terms in the actions. For this, we substitute Poincaré coordinates given by:

$$x_i = \sqrt{2Q_i} \cos q_i, \quad y_i = \sqrt{2Q_i} \sin q_i, \quad i = 1, 2, 3, \quad (43)$$

so that

$$\Gamma = \frac{1}{2} \sum_i (x_i^2 + y_i^2)$$

and, in order to harmonise the notation, define $\lambda = q_4$. Therefore, we now work with the resonant Hamiltonian

$$\mathcal{H}(\Lambda, x_i, \lambda, y_i) = \omega\Gamma - \frac{3}{2} (A\Gamma^2 + 2B\Lambda\Gamma + C\Lambda^2) + \mathcal{H}_{res}^{(1)} \quad (44)$$

where $\mathcal{H}_{res}^{(1)}$ is the resonant coupling part (16) expressed in the new variables:

$$\mathcal{H}_{res}^{(1)}(x_i, y_i, \lambda) = -\alpha x_1 - \beta_1 x_2 - \beta_2 (x_2 \cos \lambda + y_2 \sin \lambda) - \gamma (x_3 \cos \lambda + y_3 \sin \lambda). \quad (45)$$

To consider in (44) $\mathcal{H}_{res}^{(1)}$ of the same order as \mathcal{H}_1 is a bit in contrast with the new book-keeping imposed by (36-37), but is nonetheless essential to get meaningful equations for the critical points.

Let us denote with X_i, Y_i, A_E, λ_E the equilibrium values of the eccentricity vectors x_i, y_i and of the pair A, λ . From Hamiltonian (44), the equilibrium values are given by solving the systems of equation

$$\dot{A} = 0 \rightarrow \frac{\partial \mathcal{H}}{\partial \lambda} = 0 \rightarrow \beta_2(-x_2 \sin \lambda + y_2 \cos \lambda) + \gamma(-x_3 \sin \lambda + y_3 \cos \lambda) = 0 \quad (46)$$

$$\dot{\lambda} = 0 \rightarrow \frac{\partial \mathcal{H}}{\partial A} = 0 \rightarrow C\Lambda + B\Gamma = 0 \quad (47)$$

and $\dot{x}_i = 0$ and $\dot{y}_i = 0$ respectively giving

$$\begin{aligned} (3A\Gamma + 3B\Lambda - \omega)y_1 &= 0 \\ (3A\Gamma + 3B\Lambda - \omega)y_2 + \beta_2 \sin \lambda &= 0 \\ (3A\Gamma + 3B\Lambda - \omega)y_3 + \gamma \sin \lambda &= 0 \end{aligned} \quad (48)$$

and

$$\begin{aligned} (3A\Gamma + 3B\Lambda - \omega)x_1 + \alpha &= 0 \\ (3A\Gamma + 3B\Lambda - \omega)x_2 + \beta_1 + \beta_2 \cos \lambda &= 0 \\ (3A\Gamma + 3B\Lambda - \omega)x_3 + \gamma \cos \lambda &= 0. \end{aligned} \quad (49)$$

The solutions of the combined set given by (46) and (48) are given by $Y_j = 0$ and by $\lambda_E = 0, \pi$ so that (49) now become

$$\begin{aligned} (2K\Gamma_E - \omega)X_1 - \alpha &= 0 \\ (2K\Gamma_E - \omega)X_2 - \beta_1 \mp \beta_2 &= 0 \\ (2K\Gamma_E - \omega)X_3 \mp \gamma &= 0 \end{aligned} \quad (50)$$

where K has been defined above in (42), the *equilibrium angular momentum deficit* is

$$\Gamma_E = \Gamma|_{Y_i=0} = \frac{1}{2}(X_1^2 + X_2^2 + X_3^2)$$

and it has been exploited the relation

$$\Lambda_E = -\frac{B}{C}\Gamma_E \quad (51)$$

solution of the $\dot{\lambda} = 0$ condition (47). Upper and lower signs respectively refer to the ‘de Sitter’ ($\lambda_E = \pi$) and ‘anti-de Sitter’ ($\lambda_E = 0$) equilibria.

The exact solutions of the system of equations (50) are found in the following way. We assume $X_j \neq 0, \forall j = 1, 2, 3$. The consistency of this assumption is checked in the end but is justified by the above discussion concerning ω . From the quotient of each equation of the system by X_j , we get the chain of equalities

$$K(X_1^2 + X_2^2 + X_3^2) = \omega - \frac{\alpha}{X_1} = \omega - \frac{\beta_1 \mp \beta_2}{X_2} = \omega - \frac{\mp \gamma}{X_3}.$$

From the last two we get

$$X_2 = \frac{\beta_1 \mp \beta_2}{\alpha} X_1, \quad X_3 = \frac{\mp \gamma}{\alpha} X_1, \quad (52)$$

which, when inserted into the first equality, give

$$\frac{\alpha}{X_1} = \omega - K(X_1^2 + X_2^2 + X_3^2) = \omega - \hat{K}X_1^2,$$

where

$$\hat{K} = \frac{K(\alpha^2 + (\beta_1 \mp \beta_2)^2 + \gamma^2)}{\alpha^2}. \quad (53)$$

Therefore, to find exact solutions for the equilibria we have to solve the standard cubic

$$X_1^3 - \frac{\omega}{\hat{K}}X_1 + \frac{\alpha}{\hat{K}} = 0.$$

The cubic equation has the three solutions

$$X_E = \left(-\frac{\alpha}{2\hat{K}} + \sqrt{\Delta}\right)^{1/3} + \left(-\frac{\alpha}{2\hat{K}} - \sqrt{\Delta}\right)^{1/3}, \quad \Delta \doteq \frac{\alpha^2}{4} - \frac{\omega^3}{27\hat{K}}.$$

All of them are real if $\Delta \leq 0$. Therefore, interpreting the discriminant as a function of the resonance proximity parameter, the value ω_b such that $\Delta(\omega_b) = 0$ determines a *bifurcation* from one to three critical points of the reduced Hamiltonian. Therefore, for

$$\omega \geq \omega_b = \left(\frac{27}{4}\alpha^2\hat{K}\right)^{1/3} = \left(\frac{27K}{4}(\alpha^2 + (\beta_1 \mp \beta_2)^2 + \gamma^2)\right)^{1/3}, \quad (54)$$

‘New-de Sitter equilibria’ will appear (Pucacco 2021). Explicitly, we have

$$\begin{aligned} X_{1E} &= \left[\frac{\alpha}{2\hat{K}} \left(-1 + \sqrt{1 - \left(\frac{\omega}{\omega_b}\right)^3} \right) \right]^{1/3} + \left[\frac{\alpha}{2\hat{K}} \left(-1 - \sqrt{1 - \left(\frac{\omega}{\omega_b}\right)^3} \right) \right]^{1/3}, \\ X_{2E} &= \frac{\beta_1 \mp \beta_2}{\alpha} X_{1E}, \\ X_{3E} &= \pm \frac{\gamma}{\alpha} X_{1E}. \end{aligned} \quad (55)$$

Since $\omega_b > 0$, (54) says that bifurcation occurs only in the quite extreme cases of positive resonance offsets or for large values of forced eccentricities.

For sake of convenience it can be useful to re-derive the first-order approximation of the relative equilibria of the system. Coming back to the original book-keeping providing the ordering of the Hamiltonian as in (33-35), we get the following conditions for the critical points:

$$\begin{aligned} \omega y_1 &= 0 \\ \omega y_2 - \beta_2 \sin \lambda &= 0 \\ \omega y_3 - \gamma \sin \lambda &= 0. \end{aligned} \quad (56)$$

and

$$\begin{aligned} \omega x_1 - \alpha &= 0 \\ \omega x_2 - \beta_1 - \beta_2 \cos \lambda &= 0 \\ \omega x_3 - \gamma \cos \lambda &= 0. \end{aligned} \quad (57)$$

The solutions are still

$$y_i \doteq Y_i = 0, \quad \forall i = 1, 2, 3, \quad (58)$$

and:

$$\begin{aligned} x_1 &\doteq X_1^A = \frac{\alpha}{\omega} \\ x_2 &\doteq X_2^A = \frac{\beta_1 \mp \beta_2}{\omega} \\ x_3 &\doteq X_3^A = \mp \frac{\gamma}{\omega} \end{aligned} \quad (59)$$

where, as before, the upper sign corresponds to the ‘de-Sitter’ equilibrium value $\lambda_E = \pi$ and the lower sign corresponds to the ‘anti-de-Sitter’ equilibrium $\lambda_E = 0$. The apex A stands for *asymptotic* meaning that, as we can see comparing with exact solutions, they are valid for large values of $|\omega|$.

Since all solutions are characterised by $Y_i = 0$, from the definitions (43) we see that $q_{iE} = 0, \pi$ according to the sign of X_i , whereas their absolute values provide the forced eccentricities according to

$$e_i = \frac{|X_i|}{\sqrt{L_i}}, \quad i = 1, 2, 3.$$

We remark the presence of the frequency (42) in the denominators of the solutions X_i^A . Therefore, when trying to extend the validity of the solutions to small values of ω we notice the implicit contradiction of diverging values of the eccentricity breaking the assumption at the basis of the first-order treatment. However, for small eccentricities these solutions are quite accurate and essentially coincide with those obtained by Sinclair (1975).

3.3 Equilibria: an approximate evaluation

It can be useful to find some simple approximation to the solution (55). We will proceed in two steps of increasing accuracy. We check that, if $|\omega| \gg 2\Gamma_E$, since $K \sim |\mathcal{O}(1)|$, we recover solutions (59). On the other hand, if $\omega = 0$, we get the solutions

$$\begin{aligned} X_1^0 &= -\frac{\alpha}{k^\mp} \\ X_2^0 &= -\frac{\beta_1 \mp \beta_2}{k^\mp} \\ X_3^0 &= \pm \frac{\gamma}{k^\mp}, \end{aligned} \quad (60)$$

where

$$k^\mp = \left(K(\alpha^2 + (\beta_1 \mp \beta_2)^2 + \gamma^2) \right)^{1/3}. \quad (61)$$

A simple second-order approximation can be obtained with an exponential fit of these two sets. We get

$$X_j = X_j^0 e^{\omega/\omega_A}, \quad (j = 1, 2, 3) \quad (62)$$

where

$$\omega_A = \frac{k^\mp}{e}. \quad (63)$$

Solutions (62) are a very good approximation of the exact ones for moderate values of ω around zero.

3.4 Second-order equilibria: an approximate solution including 2nd-order terms in eccentricity

We remark that the possibility to get the above closed-form solution is due to truncating the resonant term to first-order in eccentricity. Actually, one (or more) of the forced eccentricities can be so big to violate the book-keeping hierarchy assumed above. In this respect, we are required to take into account also 2nd-order terms in the eccentricities, therefore including $\mathcal{H}_{res}^{(2)}(x_i, y_i, \lambda)$, namely (8) expressed in terms of the new coordinates.

In this more general case, in view of the presence of non-diagonal terms in the system of equations (due to the quadratic couplings in the Poincaré variables given by (8)), it is no longer possible to obtain the explicit solution written above. In Pucacco (2021) we looked for solutions of the form $X_1 = X_1^{(0)} + \epsilon X_1^{(1)}$ by making the hypothesis that the eccentricity of the most internal satellite is much greater than those of the other two (namely $X_1 \gg X_2, X_3$) so that the cubic equation to solve now is

$$\left(\omega - K X_1^2\right) X_1 - \epsilon(\alpha + 2\alpha_2 X_1) = 0. \quad (64)$$

To order zero in ϵ , we get the three solutions

$$X_1^{(0)} = 0$$

and

$$X_1^{(0)} = \pm \sqrt{\frac{\omega}{K}}.$$

The first of these provides again $X_1^{(1)} = \alpha/\omega = X_1^A$, namely (59) already obtained above. But, if the argument of the square root is positive, we obtain two additional sets of solutions:

$$\begin{aligned} X_{1E}^{(N)} &= \pm \frac{\omega - \alpha_2}{\sqrt{K\omega}} - \frac{\alpha}{2\omega}, \quad N = 2, 3. \\ X_{2E}^{(N)} &= \frac{\beta_1 \mp \beta_2 + \alpha_{12} X_1^{(N)}}{\omega - 2\beta_{12} - K(X_1^{(N)})^2} \\ X_{3E}^{(N)} &= \frac{\mp \gamma}{\omega - 2\gamma_2 - K(X_1^{(N)})^2} \end{aligned} \quad (65)$$

Numerically, this approximate set is in substantial agreement with the exact solution (55) for $|\omega|$ not too small with the advantage of incorporating the 2nd-order coefficients which can play a determining role in fixing the signs of the solutions and as a consequence the values (0 or π) of the libration centres. They are:

$$\alpha_2 \doteq \frac{\bar{m}_2^2 \varepsilon_2 f_{12,3}}{L_1 L_2} > 0, \quad (66)$$

$$\alpha_{12} \doteq \frac{\bar{m}_2^2 \varepsilon_2}{\sqrt{L_1 L_2^{3/2}}} (f_{12,5} + f_{12,6}), \quad (67)$$

$$\beta_{12} \doteq \frac{\bar{m}_2^2 \varepsilon_2 f_{12,4}}{L_2^3} + \frac{\bar{m}_2 \bar{m}_3^2 \varepsilon_3 f_{23,3}}{L_3^2 L_2}, \quad (68)$$

$$\gamma_2 \doteq \frac{\bar{m}_2 \bar{m}_3^2 \varepsilon_3 f_{23,4}}{L_3^3}. \quad (69)$$

3.5 Linear stability of the de Sitter equilibria

We can refine the check of the nature of the equilibria by evaluating their linear stability. If we obtain linear instability, this is sufficient for instability tout-court and we can discard the corresponding solution.

Collectively denoting with z the set (x_k, y_k, A, λ) , we consider the linear Hamiltonian equations providing the variational system (Yoder and Peale 1981)

$$\frac{d}{dt}\delta z = JH_{zz}|_E\delta z, \quad (70)$$

where J is the symplectic matrix. Looking for solutions of the form

$$\delta z = Ze^{\sigma t},$$

we have to compute the eigenvalues of the Hamiltonian matrix in (70), namely the solutions of the characteristic equation

$$\det(JH_{zz}|_E - \sigma I) = 0,$$

where I is the unit matrix. If we find at least a pair of real eigenvalues, the equilibrium is unstable.

By using the first-order solution (59) we have shown Pucacco (2021) that a pair of eigenvalues pass from pure imaginary to real for

$$\omega > \omega_U \doteq -\frac{3B^2}{C}(X_1^2 + X_2^2 + X_3^2). \quad (71)$$

When applied to the Galilean system, the numerical value of ω_U so obtained is in substantial agreement with the numerical prediction made by (Yoder and Peale 1981).

However, when implementing any of the exact or approximate forms of second-order solutions, in which there is no pronounced increase of the forced eccentricities around nominal resonance, there is no more trace of change in the nature of the eigenvalues: in the framework of the current model in which the equilibrium solution are provided by (55), the eigenvalues remain pure imaginary confirming the dynamical (Lyapunov) stability of the relative equilibria for any value of the resonance proximity parameter in the range compatible both with formation scenarios and with observations. Due to its algebraic structure, the characteristic equation is no more explicitly solvable so we will check each case with a numerical approach (see Section 5).

4 Normalisation

The construction of a normal form allows us to get an integrable approximation of the dynamics around the equilibrium. The particular structure of the starting Hamiltonian (44) requires a transformation which combines averaging and translation: the Lie-transform method (Morbiddelli 2002; Ferraz-Mello 2007) provides both with a single operation (Henrard 1984).

Suppose to start with a Hamiltonian

$$\mathcal{H} = \mathcal{H}_0(\mathbf{Q}) + \varepsilon\mathcal{H}_1(\mathbf{Q}, \mathbf{q}) + \varepsilon^2\mathcal{H}_2(\mathbf{Q}, \mathbf{q}) + \dots \quad (72)$$

where \mathcal{H}_0 is the *unperturbed* integrable part and the perturbation is given by a series ordered according to suitable assumptions on the coefficients of the expansion. In the spirit of the Lie-transform method, we pass from old variables (\mathbf{Q}, \mathbf{q}) to new variables $(\mathbf{Q}', \mathbf{q}')$ by means of a generating function $\chi_1(\mathbf{Q}', \mathbf{q}')$, such that the new Hamiltonian is

$$\begin{aligned} \mathcal{H}^{(1)}(\mathbf{Q}', \mathbf{q}') &= \mathcal{H}_0(\mathbf{Q}') + \varepsilon [\mathcal{H}_1(\mathbf{Q}', \mathbf{q}') + \{\mathcal{H}_0(\mathbf{Q}'), \chi_1(\mathbf{Q}', \mathbf{q}')\}] + \\ &\varepsilon^2 \left[\mathcal{H}_2(\mathbf{Q}', \mathbf{q}') + \{\mathcal{H}_1(\mathbf{Q}', \mathbf{q}'), \chi_1(\mathbf{Q}', \mathbf{q}')\} + \frac{1}{2} \{ \{ \mathcal{H}_0(\mathbf{Q}'), \chi_1(\mathbf{Q}', \mathbf{q}') \}, \chi_1(\mathbf{Q}', \mathbf{q}') \} \right] \end{aligned} \quad (73)$$

plus higher-order terms.

We look for a transformation such that the new Hamiltonian is *in normal form*, namely $\sum_n \varepsilon^n \mathcal{K}_n$, is constructed so to commute with the integrable part:

$$\mathcal{L}_{\mathcal{H}_0} \mathcal{K}_n \doteq \{\mathcal{K}_n, \mathcal{H}_0\} = 0, \quad \forall n. \quad (74)$$

At first order in ε , (73) gives

$$\mathcal{H}_1(\mathbf{Q}', \mathbf{q}') + \{\mathcal{H}_0(\mathbf{Q}'), \chi_1(\mathbf{Q}', \mathbf{q}')\} = \mathcal{K}_1(\mathbf{Q}'). \quad (75)$$

This is solved by equating \mathcal{K}_1 to those terms of \mathcal{H}_1 which are in the kernel of the Hamiltonian operator $\mathcal{L}_{\mathcal{H}_0}$ and using the remaining terms to integrate the generating function. Accordingly, at second order in ε , we get¹

$$\mathcal{H}^{(2)}(\mathbf{Q}', \mathbf{q}') = \mathcal{H}_2(\mathbf{Q}', \mathbf{q}') + \frac{1}{2} \{ \mathcal{H}_1(\mathbf{Q}', \mathbf{q}') + \mathcal{K}_1(\mathbf{Q}'), \chi_1(\mathbf{Q}', \mathbf{q}') \} + \{ \mathcal{H}_0(\mathbf{Q}'), \chi_2(\mathbf{Q}', \mathbf{q}') \} \quad (76)$$

from which \mathcal{K}_2 and a second generating function $\chi_2(\mathbf{Q}', \mathbf{q}')$ are computed and so forth at steps $n > 2$.

We follow above procedure by constructing a normal form for the Laplace resonance with the two book-keeping schemes discussed above. First we recall the first-order (in the integrable part) one introduced by Pucacco (2021) valid for ω far from zero. Then we introduce the normalisation scheme for the 2nd-order integrable part able to cope with the case $\omega \sim 0$.

4.1 Linear normalisation

Consider again Hamiltonian (44). Let us first adopt the book-keeping criterion introduced to treat the small-eccentricity cases (34-35) and so consider the starting Hamiltonian

$$\mathcal{H} = \omega \Gamma + \varepsilon \mathcal{H}_{res} + \varepsilon^2 \left(-3B\Lambda\Gamma - \frac{3}{2}C\Lambda^2 - \frac{3}{2}A\Gamma^2 \right). \quad (77)$$

The ω frequency is associated with the free eccentricity oscillations. We assume it to be ‘fast’ with respect to the libration of the Laplace argument. We can therefore normalise with respect to the ‘isotropic oscillator’ (Sanders et al. 2007)

$$\mathcal{H}_0 = \omega \Gamma = \omega(Q_1 + Q_2 + Q_3)$$

¹ Strictly in (76) we should distinguish the new variables from $(\mathbf{Q}', \mathbf{q}')$ denoting them with, e.g., a double prime: however, to not overwhelm the notation, we keep the usual attitude and leave the same symbol for the new variables at each step of normalisation.

by removing the dependence of the Hamiltonian on fast angles. From a quick inspection, we see that no term in $\mathcal{H}_1 = \mathcal{H}_{res}$ commutes with \mathcal{H}_0 . The solution to the first-order homological equation is therefore $\mathcal{K}_1 = 0$ and

$$\begin{aligned} \chi_1(\mathbf{Q}', \mathbf{q}') &= -\frac{\alpha}{\omega} \sqrt{2Q'_1} \sin q'_1 - \frac{\beta_1}{\omega} \sqrt{2Q'_2} \sin q'_2 \\ &\quad - \frac{\beta_2}{\omega} \sqrt{2Q'_2} \sin(q'_2 - \lambda') - \frac{\gamma}{\omega} \sqrt{2Q'_3} \sin(q'_3 - \lambda'). \end{aligned} \quad (78)$$

At second order, examining (76), the first Poisson bracket turns out to be equal to

$$-\frac{\alpha^2 + \beta_1^2 + \beta_2^2 + \gamma^2}{2\omega} - \frac{\beta_1\beta_2}{\omega} \cos \lambda',$$

so that the second homological equation has solutions $\chi_2 = 0$ and, neglecting a trivial constant term,

$$\mathcal{K}_2 = 3BA'(Q'_1 + Q'_2 + Q'_3) + \frac{3}{2}CA'^2 + \frac{3}{2}A(Q'_1 + Q'_2 + Q'_3)^2 + \frac{\beta_1\beta_2}{\omega} \cos \lambda'. \quad (79)$$

The transformed angular momentum deficit can be denoted as

$$\Gamma_E = Q'_1 + Q'_2 + Q'_3, \quad (80)$$

and, in this approximation, is a conserved quantity. Therefore, the 2nd-order normal form is equivalent to the reduced Laplace Hamiltonian (Pucacco 2021)

$$K_L(\Lambda', \lambda'; \Gamma_E) = 3B\Gamma_E\Lambda' + \frac{3}{2}C\Lambda'^2 + \frac{\beta_1\beta_2}{\omega} \cos \lambda'. \quad (81)$$

It provides a first-order approximation of the libration frequency around the reference $\lambda' = \pi$ equilibrium

$$\omega_L = \sqrt{\frac{3C\beta_1\beta_2}{\omega}} \quad (82)$$

and an approximate resonance width given by

$$\Delta\Lambda = 4\sqrt{\frac{\beta_1\beta_2}{3C\omega}}. \quad (83)$$

Another clear aspect of the dynamics in the first-order resonance cases refers to the free eccentricities. The back transformations to original variables, say \mathbf{q} , are given by series of the form $\sum_k \mathbf{q}^{(k)}$ in terms of the normalising coordinates given by

$$\mathbf{q}^{(0)} = \mathbf{q}', \quad (84)$$

$$\mathbf{q}^{(1)} = \{\mathbf{q}', \chi_1\}, \quad (85)$$

$$\mathbf{q}^{(2)} = \{\mathbf{q}', \chi_2\} + \frac{1}{2}\{\{\mathbf{q}', \chi_1\}, \chi_1\}, \quad (86)$$

$$\vdots = \vdots \quad (87)$$

Using the generating functions obtained above we get in terms of Poincaré variables

$$x_1 = x'_1 - \frac{\partial \chi_1}{\partial y'_1} = x'_1 + \frac{\alpha}{\omega}, \quad (88)$$

$$y_1 = y'_1 + \frac{\partial \chi_1}{\partial x'_1} = y'_1, \quad (89)$$

$$x_2 = x'_2 - \frac{\partial \chi_1}{\partial y'_2} = x'_2 + \frac{1}{\omega} (\beta_1 + \beta_2 \cos \lambda'), \quad (90)$$

$$y_2 = y'_2 + \frac{\partial \chi_1}{\partial x'_2} = y'_2 + \frac{\beta_2}{\omega} \sin \lambda', \quad (91)$$

$$x_3 = x'_3 - \frac{\partial \chi_1}{\partial y'_3} = x'_3 + \frac{\gamma}{\omega} \cos \lambda', \quad (92)$$

$$y_3 = y'_3 + \frac{\partial \chi_1}{\partial x'_3} = y'_3 + \frac{\gamma}{\omega} \sin \lambda', \quad (93)$$

where the ‘new’ (x'_i, y'_i) represent the free eccentricity oscillations

$$x'_i = c_i \cos \omega(t - t_0), \quad y'_i = d_i \sin \omega(t - t_0).$$

The amplitudes (c_i, d_i) are fixed by initial conditions. These relations show how the transformation to the Laplace normal form, aimed at removing non-resonant terms depending on q_i , automatically shifts the eccentricity vectors to the forced equilibria. The back transformations (88-93), when imposing the equilibrium conditions $\lambda' = 0$ or $\lambda' = \pi$, are therefore in perfect agreement with solutions (59).

4.2 Non-linear normalisation

Let us now adopt the book-keeping criterion introduced to treat the general cases (36-37) in which also large eccentricities are admitted and so consider the starting Hamiltonian (44)

$$\mathcal{H} = \mathcal{H}_0 + \varepsilon \mathcal{H}_1$$

where now the whole integrable part (including quadratic terms in the actions) is used as unperturbed Hamiltonian with respect to which to normalise (Batygin et al. 2015)

$$\mathcal{H}_0 = \omega \Gamma - \left(\frac{3}{2} A \Gamma^2 + 3 B A \Gamma \right)$$

and

$$\mathcal{H}_1 = \mathcal{H}_{res} - \frac{3}{2} C A^2.$$

Comparing with (77), this is equivalent to not considering anymore ω ‘fast’.

The solution of the first homological equation (75) now provides the generating function

$$\begin{aligned} \chi_1(\mathbf{Q}', \mathbf{q}') = & - \frac{\alpha \sqrt{2Q'_1} \sin q'_1 + \beta_1 \sqrt{2Q'_2} \sin q'_2}{\omega - 3A\Gamma' - 3BA'} + \\ & - \frac{\beta_2 \sqrt{2Q'_2} \sin(q'_2 - \lambda') + \gamma \sqrt{2Q'_3} \sin(q'_3 - \lambda')}{\omega - 3(A-B)\Gamma' - 3(B-C)A'} \end{aligned} \quad (94)$$

and we get

$$\mathcal{K}_1 = -\frac{3}{2}CA^2$$

implying the successful elimination of the harmonics of order ε . In this case however, in view of the non-linear nature of \mathcal{H}_0 , this implies the appearance in $\mathcal{H}^{(2)}(\mathbf{Q}', \mathbf{q}')$ of harmonics of order ε^2 with several new angle combinations (Morbidelli and Giorgilli 1997; Morbidelli 2002). In particular, in \mathcal{K}_2 they appear terms with $q_2 - \lambda$ and $q_3 - \lambda$ that can be used to describe ‘beats’ between ω and ω_L . For the sake of the present work its detailed form is not relevant and we limit ourself only to report the change of the librating term in $\cos \lambda$ with respect to (81)

$$\frac{\beta_1 \beta_2}{2} \left(\frac{1}{\omega - 3A\Gamma' - 3BA'} + \frac{1}{\omega - 3(A-B)\Gamma' - 3(B-C)A'} \right) \cos \lambda'$$

providing a first approximation of the effect of the non-linear terms on the pendulum dynamics. In particular, we can see how is removed the divergence in (82) and (83) when $\omega \rightarrow 0$. On the other hand, it is very interesting to compare the back transformation of the coordinates given by the generating function (94). In analogy with (88-93) we get now

$$\begin{aligned} x_1 &= x'_1 + \frac{\alpha}{\omega - 3A\Gamma' - 3BA'} \\ &\quad + \frac{3A(\alpha y'_1 + \beta_2 y'_2) y'_1}{(\omega - 3A\Gamma' - 3BA')^2} + \frac{3(A-B) [(\beta_2 y'_2 + \gamma y'_3) \cos \lambda' - (\beta_2 x'_2 + \gamma x'_3) \sin \lambda'] y'_1}{(\omega + 3(B-A)\Gamma' - 3(C-B)A')^2}, \\ x_2 &= x'_2 + \frac{\beta_1}{\omega - 3A\Gamma' - 3BA'} + \frac{\beta_2 \cos \lambda'}{\omega + 3(B-A)\Gamma' - 3(C-B)A'} \\ &\quad + \frac{3A(\alpha y'_1 + \beta_2 y'_2) y'_2}{(\omega - 3A\Gamma' - 3BA')^2} + \frac{3(A-B) [(\beta_2 y'_2 + \gamma y'_3) \cos \lambda' - (\beta_2 x'_2 + \gamma x'_3) \sin \lambda'] y'_2}{(\omega + 3(B-A)\Gamma' - 3(C-B)A')^2}, \\ x_3 &= x'_3 + \frac{\gamma \cos \lambda'}{\omega + 3(B-A)\Gamma' - 3(C-B)A'} \\ &\quad + \frac{3A(\alpha y'_1 + \beta_2 y'_2) y'_3}{(\omega - 3A\Gamma' - 3BA')^2} + \frac{3(A-B) [(\beta_2 y'_2 + \gamma y'_3) \cos \lambda' - (\beta_2 x'_2 + \gamma x'_3) \sin \lambda'] y'_3}{(\omega + 3(B-A)\Gamma' - 3(C-B)A')^2}, \end{aligned}$$

for the x_i and similar expressions for the y_i . Imposing again the equilibrium values $x'_i = 0, y'_i = 0$ (which imply (51)) and $\lambda' = 0, \pi$, we can check that we re-obtain system (50). Therefore, also in this case the procedure of Lie-transform normalisation produces the correct shift to the forced equilibria.

5 Applications

There are two case-studies that happily perfectly fit the two main occurrences of relative equilibria illustrated above in Section 3: the Galilean system is the standard example of Laplace resonance close (even if not exactly) at a de Sitter-Sinclair equilibrium; the exo-planetary system Gliese 876 is instead well described by one of the new-de Sitter equilibria. In the light of the theory discussed above, we illustrate these two examples in the following subsections. There is no claim to rigor: the aim is just to show the main aspects of these results.

5.1 The Galilean system

We use the mass-parameters of the Galilean system to investigate the corresponding family of equilibria. We remark that the model is highly idealised: in particular, the oblateness of Jupiter is neglected.

In Fig.1 we plot both the exact and approximate solutions (respectively (55) and (58-59)) to show their very different behaviour when $\omega \rightarrow 0$. The verse of the proximity parameter is reversed in order to easily compare these solutions with the classical results published in Yoder and Peale (1981) and Henrard (1982). We refer to eq.(42) to recall the connection between the proximity parameter and the resonance offsets used in those references: in particular, Henrard (1982) adopts the same units of measures used here (Pucacco 2021), showing a good agreement with our approximate solutions. In Fig.2 we also perform the comparison between the analytical solutions (55) and the exponential fit (62).

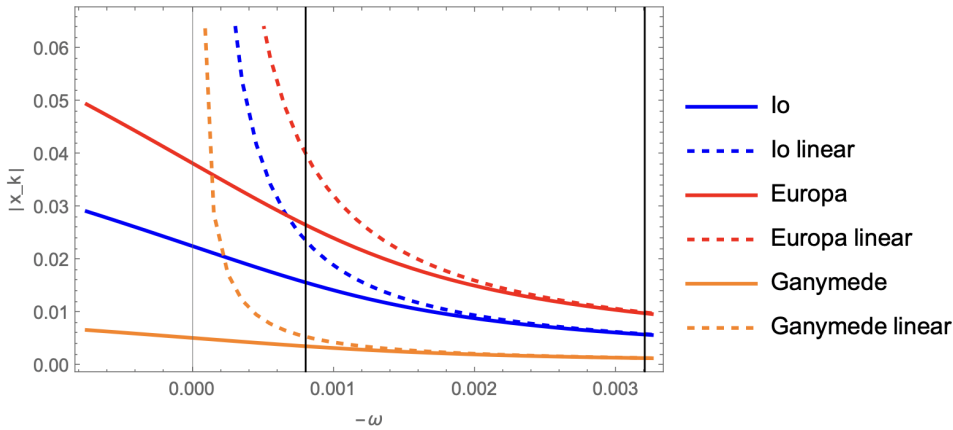


Fig. 1 De Sitter-Sinclair equilibria for the Galilean system: continuous lines correspond to solution (55); dashed lines to the approximate solutions (58-59). The verse of the proximity parameter ω is reversed. The vertical thick lines give the actual observed value ($\omega = -0.00325$) and the instability threshold ($\omega = -0.00078$) predicted by applying (71).

In Fig.3 we compare the analytical solutions (55) with exact solutions obtained by a root-finding method of the complete model including 2nd-order terms in eccentricity. The verse of the proximity parameter is now the standard one; moreover, we can also see the sign of each solution which, according to the definition of Poincaré variables, determines the value of the libration centre for each resonant angle.

Finally, in the following tables we report the eigenvalues of the stability matrix at equilibrium: in Table 1 we have the case very close to the actual state of the Galilean system ($Q_5 = 1.2259$, $Q_6 = 4.3199$, $\omega = -0.00325$), respectively using the first and the 2nd-order solutions; in Table 2, that corresponding to a configuration deep in resonance, ($Q_5 = 1.2257$, $Q_6 = 4.3127$, $\omega = -0.00075$), which according to the first-order theory should be (and indeed is not) dynamically unstable.

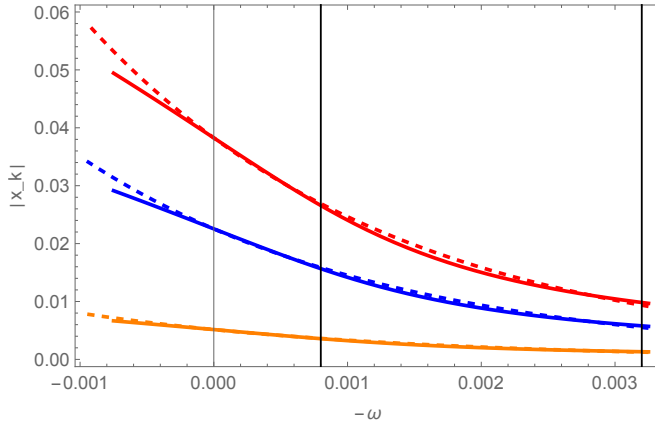


Fig. 2 De Sitter-Sinclair equilibria for the Galilean system: comparison between the analytical solutions (55, continuous lines) and the exponential fit (62, dashed lines). The color code is the same as in Fig.1

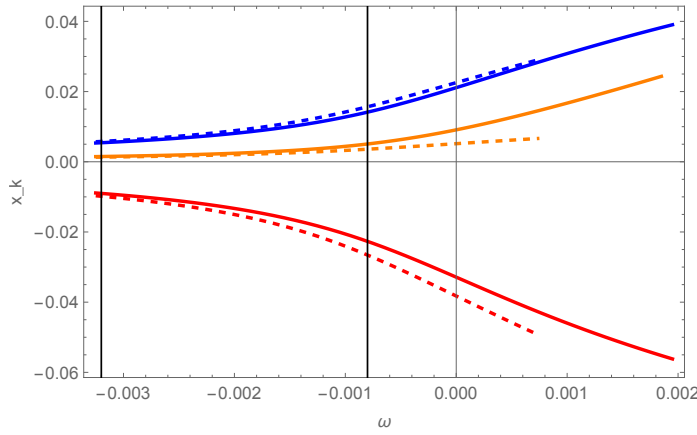


Fig. 3 De Sitter-Sinclair equilibria for the Galilean system: comparison between the analytical solutions (55), dashed lines, and exact solutions obtained by a root-finding method of the complete model including the 2nd-order terms in eccentricity (continuous lines). The color code is the same as in Fig.1.

5.2 GJ-876

The system Gliese-Jahreiß 876 (GJ-876) is very important because it was the first case of discovery of mean motion-resonance outside our Solar System (Marcy et al. 2001) and of multi-resonance among three planets (Rivera et al. 2010). In Table 3 we list the nominal elements reported in Nelson et al. (2016). Semi-major axes and eccentricities are quite well known, with $e_1 = 0.2531$ for the first planet in the chain, planet-c, a Jupiter-like with a period of 30 days. A second Jupiter, planet-b (since it was the first to be discovered) has a period of 61 days and finally there is a Uranus-like object, planet-e, with a period of 124.5 days.

eigenvalues	Analytical 1st-order	Analytical 2nd-order	Numerical
σ_2	0.00111 <i>i</i>	0.00096 <i>i</i>	0.00086 <i>i</i>
σ_4	0.00284 <i>i</i>	0.00392 <i>i</i>	0.00390 <i>i</i>
σ_6	0.00352 <i>i</i>	0.00423 <i>i</i>	0.00400 <i>i</i>
σ_8	0.00369 <i>i</i>	0.00534 <i>i</i>	0.00463 <i>i</i>

Table 1 Galilean system (observed): $Q_6 = 4.3199, \omega = -0.00325$.

eigenvalues	Analytical 1st-order	Analytical 2nd-order	Numerical
σ_2	0.00448	0.00061 <i>i</i>	0.00070 <i>i</i>
σ_4	0.00056 <i>i</i>	0.00082 <i>i</i>	0.00129 <i>i</i>
σ_6	0.00075 <i>i</i>	0.00141 <i>i</i>	0.00161 <i>i</i>
σ_8	0.00353 <i>i</i>	0.00333 <i>i</i>	0.00213 <i>i</i>

Table 2 Galilean system (closer to resonance): $Q_6 = 4.3127, \omega = -0.00075$.

semi-major axis [in unit of a_1]	Planet c	Planet b	Planet e				
nominal	1	1.6074	2.5840				
de Sitter-Sinclair	1	1.6093	2.6350				
new de Sitter	1	1.6052	2.5829				
eccentricity/resonant angles	e_1	e_2	e_3	q_1	q_2	q_3	q_4
observed	0.2531	0.0368	0.0310	0	0	rotating?	0
de Sitter-Sinclair ($X_k^A(\pi)$)	0.0480	0.0047	0.0064	π	0	0	π
de Sitter-Sinclair ($X_k^A(0)$)	0.0524	0.0104	0.0023	π	0	0	0
new de Sitter ($X_k(\pi)$)	0.2657	0.0737	0.0117	0	π	π	π
new de Sitter ($X_k(0)$)	0.2546	0.0366	0.0381	0	0	π	0

Table 3 Mean nominal orbital elements of the 3 main planets in GJ-876 and resonant angles according to Nelson et al. (2016) compared with predictions from the model.

A remarkable aspect of this configuration concerns the possibility to have *triple conjunctions*: in the lower panel of Fig. 4 it can be seen that these configurations are allowed (Rivera et al. 2010) with planet-c and -b at periastron ($\lambda_1 = \lambda_2 = p_1 = p_2 = 0$) and planet-e at apastron ($\lambda_3 = 0, p_3 = \pi$). On the other hand, in the Galilean case Europa and Ganymede can only be in conjunction with Io one at a time.

GJ-876 is then the prototype of systems in which the new de Sitter equilibria appear to be in very good agreement with observation. It is clearly stimulating to try to understand these results in the framework of the theory of resonant capture (Charalambous et al. 2018; Pichierri et al. 2019) and also to get clues about the structure of the other systems for which less accurate informations are available.

The bifurcation value of the proximity parameter, when upgraded with the complete 2nd-order terms is

$$\omega'_b = \omega_b + 2\alpha_2 = 0.0909.$$

Inserting the observed data, it appears that the current status of the system corresponds to $\omega = 0.1159$, so that it is beyond the bifurcation threshold. Therefore, the solution which best describes the actual system is indeed the stable branch after the saddle-node bifurcation of the sequence with libration center of the Laplace argument at $\lambda = q_4 = 0$. In Figs. 5-7 we plot the exact 2nd-order solutions computed with a root-finding method. We can see a close similarity with the equilibria obtained by Batygin (2015) in the case of the 2-planet MMR case. The bifurcation threshold computed above seems to be quite accurate: note that also here the usual verse of the

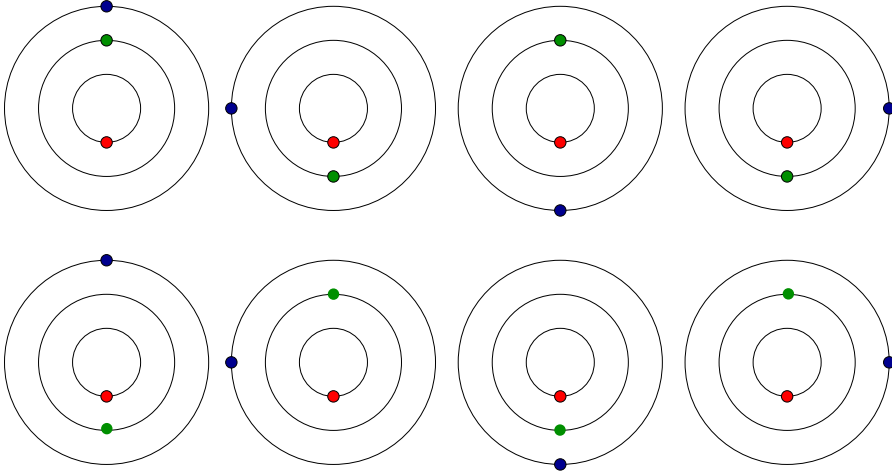


Fig. 4 Idealised pictures of the Galilean system (top panel) compared with GJ-876 (lower panel). Each snapshot corresponds to a revolution period of Io or planet-c (red dots); in the upper plots Europa (green dots) and Ganymede (blue dots) can be in conjunction with Io one at a time; in the lower plots, planet-b (green dots) and planet-e (blue dots) can together be in conjunction with planet-c.

abscissa-axis is used. Comparing with values reported in Table 3, we can verify how also the apsidal configuration is correctly reconstructed by the new de Sitter family with $\lambda = 0$.

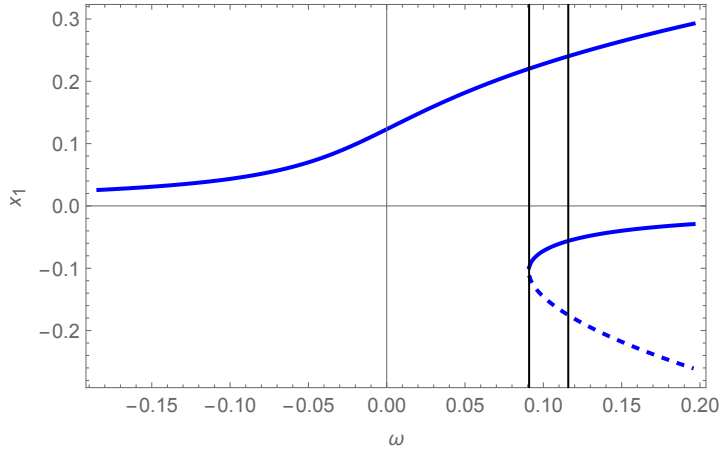


Fig. 5 New deSitter for the GJ-876 system: X_1 solutions with $\lambda = 0$. The vertical thick lines give the actual observed value ($\omega = 0.1159$) and the bifurcation threshold ($\omega = 0.0909$).

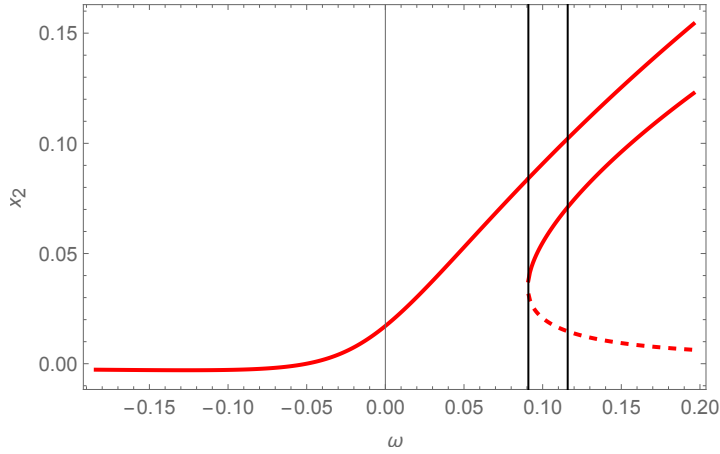


Fig. 6 Same as Fig.5: X_2 solutions.

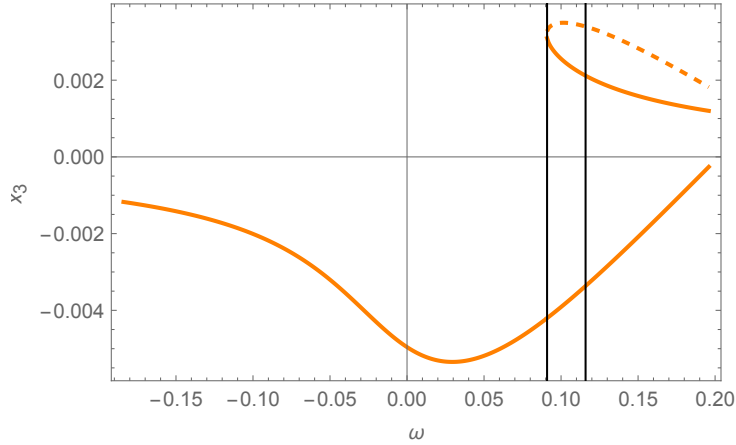


Fig. 7 Same as Fig.5: X_3 solutions.

6 Conclusions

We can summarise the results of the present work with the following remarks:

1. The sequence of Laplace-resonant equilibrium configurations can be parametrised by a single frequency (the ‘resonance proximity parameter’) depending on the two integrals of motion admitted by the Hamiltonian model.
2. The equilibrium is dynamically (Lyapunov) stable all along the sequence up to a threshold determining a saddle/node bifurcation with two additional stable/unstable sequences.
3. The range of models in which the resonance proximity parameter is close to vanishing require a proper ordering of the Hamiltonian series which impacts on the construction of the resonant normal form governing the dynamics around the equilibrium.

The simple model in which only first-order resonant terms are considered allows us to get explicit solutions for the equilibrium sequence and the bifurcation threshold. It

is qualitatively correct also for what concerns the apsidal configurations. To get more accurate quantitative results, the inclusion of higher-order terms requires numerical root-finding methods.

There are at least two straightforward extensions of this work that can be proposed for further study: first, a systematic investigation of the equilibrium sequences by varying the physical parameters (in particular the mass-ratios); second, to exploit the non-linear normal form to study higher-order harmonics in the perturbations.

Acknowledgements

I acknowledge the ASI Contract n. 2023-6-HH.0 (Scientific Activities for JUICE, E phase) and partial support from GNFM/INdAM and INFN (Sezione di RomaII).

Compliance with ethical standards

Conflict of interest: The author declares that he has no conflict of interest.

References

- Abraham R, Marsden JE (1987) Foundations of Mechanics. The Benjamin/Cummings Publ. Co., Reading, MA
- Batygin K (2015) Capture of planets into mean-motion resonances and the origins of extrasolar orbital architectures. *Monthly Notices of the Royal Astronomical Society* 451:2589–2609
- Batygin K, Morbidelli A (2013a) Analytical treatment of planetary resonances. *Astronomy and Astrophysics* 556:A28
- Batygin K, Morbidelli A (2013b) Dissipative divergence of resonant orbits. *Astronomical Journal* 145:1
- Batygin K, Morbidelli A, Holman MJ (2015) Chaotic disintegration of the inner Solar system. *Astrophysical Journal* 799:120–136
- Broer HW, Hanßmann H (2016) On Jupiter and his Galilean satellites: Librations of de Sitter’s periodic motions. *Indagationes Mathematicae* 27:1305–1336
- Capuccio P, Hickey A, Durante D, Di Benedetto M, Iess L, De Marchi F, Plainaki C, Milillo A, Mura A (2020) Ganymede’s gravity, tides and rotational state from JUICE 3GM experiment simulation. *Planet Space Sci* 104902:187
- Celletti A, Paita F, Pucacco G (2019) The dynamics of Laplace-like resonances. *Chaos: An Interdisciplinary Journal of Nonlinear Science* 29(3):033111
- Charalambous C, Martì JG, Beaugé C, Ramos XS (2018) Resonance capture and dynamics of three-planet systems. *Monthly Notices of the Royal Astronomical Society* 477:1414–1425
- Charalambous C, Teyssandier J, Libert AS (2023) Tidal interactions shape period ratios in planetary systems with three-body resonant chains. *Astronomy and Astrophysics* 677:A160
- Couturier J, Robutel P, Correia ACM (2022) Dynamics of co-orbital exoplanets in a first order resonance chain with tidal dissipation. *Astronomy and Astrophysics* 664:A1
- de Sitter W (1909) On the periodic solutions of a special case of the problem of four bodies. *Proceedings of the Roy Acad Sci Amsterdam* 11:682–698
- de Sitter W (1931) Jupiter’s Galilean satellites (George Darwin Lecture). *Monthly Notices of the Royal Astronomical Society* 91:706–738
- Delisle JB (2017) Analytical model of multi-planetary resonant chains and constraints on migration scenarios. *Astronomy and Astrophysics* 605:A96
- Ferraz-Mello S (2007) Canonical Perturbation Theories, Degenerate Systems and Resonance. Springer Science and Business Media, New York
- Ferraz-Mello S (2021) Dynamics of the Galilean Satellites: An Introductory Treatise. Open Access revised edition. Instituto Astronomico e Geofisico, Universidade de São Paulo

- Goldberg M, Batygin K, Morbidelli A (2022) A criterion for the stability of planets in chains of resonances. *Icarus* 388:115206
- Henrard J (1982) Orbital Evolution of the Galilean Satellites: The Conservative Model, Proceedings of the Sao Paulo Conference, The motion of Planets and Natural and Artificial Satellites, Edited by S. Ferraz-Mello and P. E. Nacozy, Reidel, Dordrecht, pp 233–244
- Henrard J (1984) Libration of Laplace’s argument in the Galilean satellites theory. *Cel Mech* 34:255–262
- Izidoro A, Ogihara M, Morbidelli A (2017) Breaking the chains: hot super-Earth systems from migration and disruption of compact resonant chains. *Monthly Notices of the Royal Astronomical Society* 470:1750–1770
- Lainey V, Duriez L, Vienne A (2006) Synthetic representation of the Galilean satellites’ orbital motions from L1 ephemerides. *Astronomy and Astrophysics* 456:783–788
- Lari G, Saillenfest M (2024) The nature of the Laplace resonance between the Galilean moons. *Celest Mech Dyn Astr* 136(–):19
- Laskar J, Petit AC (2017) AMD-stability and the classification of planetary systems. *Astronomy and Astrophysics* 605:A72
- Malhotra R (1991) Tidal origin of the Laplace resonance and the resurfacing of Ganymede. *Icarus* 94(2):399–412
- Marcy GW, Butler RP, Fischer D, Vogt SS, Lissauer JJ, Rivera EJ (2001) A Pair of Resonant Planets Orbiting GJ 876. *Astrophysical Journal* 556:296
- Michtchenko TA, Beaugé C, Ferraz-Mello S (2008) Dynamic portrait of the planetary 2/1 mean-motion resonance - I. Systems with a more massive outer planet. *Monthly Notices of the Royal Astronomical Society* 387:747–758
- Morbidelli A (2002) *Modern Celestial Mechanics*. Taylor and Francis
- Morbidelli A, Giorgilli A (1997) On the role of high order resonances in normal forms and in separatrix splitting. *Physica D* 102:195–207
- Murray CD, Dermott SF (2000) *Solar System Dynamics*. Cambridge University Press
- Nagpal V, Goldberg M, Batygin K (2024) Breaking Giant Chains: Early-stage Instabilities in Long-period Giant Planet Systems. *Astrophysical Journal* 969:133
- Nelson BE, Robertson PM, Payne M, et al (2016) An Empirically Derived Three-Dimensional Laplace Resonance in the Gliese-876 Planetary System. *Mon Not Roy Astron Soc* 455:2484–2499
- Papaloizou JCB (2015) Three body resonances in close orbiting planetary systems: tidal dissipation and orbital evolution. *International Journal of Astrobiology* 14:291–304
- Petit AC, Pichierri G, Davies M, Johansen A (2020) The path to instability in compact multi-planetary systems. *Astronomy and Astrophysics* 641:A176
- Pichierri G, Morbidelli A (2020) The onset of instability in resonant chains. *Monthly Notices of the Royal Astronomical Society* 494:4950–4968
- Pichierri G, Batygin K, Morbidelli A (2019) The role of dissipative evolution for three-planet, near-resonant extrasolar systems. *Astronomy and Astrophysics* 625:A7
- Pucacco G (2021) Normal forms for the Laplace resonance. *Celest Mech Dyn Astr* 133(3):11
- Rivera EJ, Lissauer JJ, Butler RP, et al (2010) The Lick-Carnegie Exoplanet Survey: a Uranus-mass fourth planet for GJ 876 in an extrasolar Laplace configuration. *Astrophysical Journal* 719:890–899
- Sanders JA, Verhulst F, Murdock J (2007) *Averaging Methods in Nonlinear Dynamical Systems*. Springer-Verlag, Berlin Heidelberg
- Sinclair AT (1975) The orbital resonances amongst the Galilean satellites of Jupiter. *Monthly Notices of the Royal Astronomical Society* 171:59–72
- Wang X, Zhou LY, Beaugé C (2024) Resonant chains in triple-planet systems. *Astronomy and Astrophysics* 687:A266
- Yoder CF, Peale SJ (1981) The Tides of Io. *Icarus* 47:1–35, (YP81)